




Heterotopic Implantation of Decellularized Pulmonary Artery Homografts In A Rodent Model: Technique Description and Preliminary Report


Arben Dedja, Massimo A. Padalino, Mila Della Barbera, Cosimo Rasola, Paola Pesce, Anna Milan, Michela Pozzobon, David Sacerdoti, Gaetano Thiene & Giovanni Stellin

To cite this article: Arben Dedja, Massimo A. Padalino, Mila Della Barbera, Cosimo Rasola, Paola Pesce, Anna Milan, Michela Pozzobon, David Sacerdoti, Gaetano Thiene & Giovanni Stellin (2017): Heterotopic Implantation of Decellularized Pulmonary Artery Homografts In A Rodent Model: Technique Description and Preliminary Report, Journal of Investigative Surgery, DOI: [10.1080/08941939.2017.1320456](https://doi.org/10.1080/08941939.2017.1320456)

To link to this article: <http://dx.doi.org/10.1080/08941939.2017.1320456>

 Published online: 08 May 2017.

 Submit your article to this journal [↗](#)

 View related articles [↗](#)

 View Crossmark data [↗](#)

Heterotopic Implantation of Decellularized Pulmonary Artery Homografts In A Rodent Model: Technique Description and Preliminary Report

Arben Dedja,¹ Massimo A. Padalino,² Mila Della Barbera,¹ Cosimo Rasola,³ Paola Pesce,⁴ Anna Milan,⁵ Michela Pozzobon,⁵ David Sacerdoti,⁴ Gaetano Thiene,¹ Giovanni Stellin^{1,2}

¹Department of Cardiac, Thoracic and Vascular Sciences, University of Padova, Padua, Italy, ²Pediatric and Congenital Cardiovascular Surgery Unit, Centro V. Gallucci, Padova University Hospital, Padua, Italy, ³University of Padova Medical School, Padua, Italy, ⁴Department of Medicine, University of Padova, Padua, Italy, ⁵Stem Cells and Regenerative Medicine Laboratory, Fondazione Istituto di Ricerca Pediatrica Città della Speranza, Padua, Italy

ABSTRACT

Purpose: Despite a substantial amount of literature on tissue-guided regeneration, decellularization process, repopulation time points and stem cell turnover, more in-depth study on the argument is required. Currently, there are plenty of reports involving large animals, as well as clinical studies facing cardiac repair with decellularized homografts, but no exhaustive rodent models are described. The purpose of this study was to develop such a model in rats; preliminary results are also herein reported. **Material and Methods:** Fresh or decellularized pulmonary homografts from wild type rats were implanted in the abdominal aorta of green fluorescent protein positive rats. Three experimental groups were build up: sham, fresh homograft recipients and decellularized homograft recipients. The homograft decellularization process was performed with three cycles of detergent-enzymatic treatment protocol. Surgical technique of pulmonary homograft implantation and postoperative ultrasonographic evaluation were also reported; gross, histology and immunohistochemistry analysis on unimplanted and postoperative homografts were also carried out. **Results:** The median total recipient operating time was 148 minutes, with a surgical success rate of 82%. The decellularization protocol resulted effective and showed a complete decellularization with intact extracellular matrix. At 15 days from surgery, the implanted decellularized pulmonary homografts exhibited cell repopulation in the outer media wall and partial endothelial lining in absence of rejection. **Conclusions:** Our technique is a feasible and reproducible model that can be fundamental for building a valid study for further exploitation on the field. Even in a short-term follow up, the decellularized pulmonary homografts showed autologous repopulation in absence of rejection.

Keywords: microsurgery; implant technique; decellularization; pulmonary homografts; rat model

INTRODUCTION

Tissue engineering techniques with decellularized scaffolds based on the principle of *in vitro* and/or *in vivo* repopulation with autologous cells can provide a valid approach to substitutive and regenerative medicine. In particular, extracellular matrix (ECM) derived scaffolds have been successfully used to repair a variety of damaged or diseased tissues, and attempts to repair cardiac valves in the preclinical setting have been

reported [1]. Current heart valve substitutes present several limitations; their most important drawback is the lack of regeneration potential and, therefore, they do not grow, repair, and remodel properly after implantation [2, 3]. The great advantage of using a biological scaffold is based on the fact that decellularized matrices closely resemble the native tissue and thus can grow and adapt in response to changing functional demands [4, 5]. In particular, ECM plays a pivotal role in tissue maintenance and regeneration, and modulates

Received 6 February 2017; accepted 12 April 2017.

Address correspondence to Arben Dedja, MD, PhD, Dipartimento di Scienze Cardiologiche, Toraciche e Vascolari, Centro "V. Gallucci", Via Giustiniani 2 – 35128 Padova, Italy. E-mail: arben.dedja@unipd.it

Color versions of one or more of the figures in the article can be found online at www.tandfonline.com/iivs.

cell adhesion and migration, growth factor storage and release, stem cell activation and differentiation [6].

Tissue engineered heart valves have shown encouraging results in preclinical large animal models and in a clinical setting [7]. Decellularization leads to considerably less deterioration in the valve allografts after implantation in the aortic or pulmonary position in juvenile sheep, compared to non-treated allografts [8, 9].

To the best of our knowledge, thorough experimental studies on decellularized pulmonary homograft implantation in small animal models (rats and mice) have not been reported, as in the case of decellularized aortic valve implants [10]. This may be because of the fact that, despite these models being less expensive when compared with the more demanding large animal models, the model is a surgically challenging one, due to technical difficulties related to small dimensions and delicate tissue.

Although several unanswered questions and controversies regarding tissue-guided regeneration (i.e. autologous cell repopulation time points, stem cell turnover, and macrophage activation) still exist, we have developed a surgical model of heterotopic decellularized pulmonary homograft (DPH) implantation in a rodent model.

The aim of this investigation was to describe in detail our model of heterotopic implantation of DPH from wild-type donor rats to the abdominal aorta of outbred green fluorescent protein positive (GFP+) recipient rats. The surgical technique was also described with improvements, adaptations, tips, and further modifications in comparison with other studies on the field. Furthermore, we aimed to verify the effectiveness of the decellularization procedure that we have used and give a histologic evaluation of the graft tissue after a short follow up.

MATERIALS AND METHODS

Animals

All surgical procedures and animal husbandry were carried out in strict accordance with the recommendations in the Guide for the Care and Use of Laboratory Animals of the National Institutes of Health. The study was approved by the University of Padua Animal Care Committee (CEASA, protocol number 666/96) and communicated to the Ministry of Health, in accordance with the Italian Law. The study involved 13 young adult wild type Sprague Dawley (SD) rats, weighing 140–210 g (donors), for the experimental groups where homograft implantation was planned, and 17 adult male or female GFP+ SD rats weighing 320–430 g (recipients). Donors and recipients were randomly matched and 17 consecutive surgical procedures performed. Recipients were divided into three

experimental groups: sham-operated group (SHAM, $n = 4$), fresh homograft group (FRESH, $n = 6$) and decellularized homograft group (DECELL, $n = 4$). The other three recipients died due to surgical complications and did not enter any experimental group. All animals were kept in conventional facilities with free access to food and water.

Instruments and Sutures

A basic set of microsurgical instruments was used, including fine-tip curved micro scissors (AE/OC497R), a Barraquer micro needle holder (AE/FD230R), two micro-jewelers forceps (straight: RU 4240-04 and curved: RU 4240-06) and two Yasargil standard clips (AE/FE752K). A ring tip micro forceps (RU 4079-14) and micro spring scissors (RU 2380-14) completed the set. A regular operating microscope M400 E (Leica Microsystems Italia Srl, Milan, Italy) was used, with $\times 10$, $\times 16$ and $\times 25$ in-procedure interchangeable magnifications. The key sutures were performed with Prolene 10/0 with BV75-3 needle (Johnson & Johnson Medical SpA, Pomezia, Italy). Silk 6/0 (Johnson & Johnson Medical SpA) was used for arterial branch ligation.

Anesthesia

A Fluovac Sevoflurane/Halotane Scavenger unit (Harvard Apparatus Ltd, Kent, UK) with an absorber filter was connected to the animal throughout the procedure. The donor, as well as the recipient rat, was injected with 5 mg/kg of intraperitoneal tramadol (Contramal[®], Formenti Srl, Milan, Italy) 15 minutes prior to surgery. Sevoflurane (Sevorane[®], Abbott SpA, Campoverde, Italy) at 4% with oxygen 1 liter per minute was supplied to a Plexiglas chamber used for anesthesia induction. Sevoflurane at 2–2.5% with oxygen 1 liter per minute was subsequently used as maintenance anesthesia. The animal muzzle was inserted in the inner tube of the unit, which served as a mask, while the excess vapor was scavenged via the outer tube.

Surgery and Decellularization

The operation was performed under clean conditions. A single surgeon carried out all the surgical and other *in vivo* procedures described here.

Donor Operation

An accurate harvesting technique proves to be crucial to the success of the implant into the recipient. The homograft requires very gentle handling during surgery. It was never touched directly and cotton buds were used to move the graft.

The donor rat was laid on a cork tray with the caudal part towards the surgeon and a xiphopubic incision with lateral openings was performed. The two superior musculocutaneous flaps were retracted laterally over the thorax. A volume of 1 mL of saline solution at 4°C containing 500 IU of heparin was administered through the abdominal vena cava (AVC). After 1 minute, the diaphragm was cut from left to right and the heart freed from the anterior thoracic wall. A wide bilateral thoracotomy was performed, cutting the posterior ribs near the spine with large scissors. The beating heart was cooled by dripping saline solution at 4°C over the organ. From then on, donor surgery was performed under $\times 10$ and $\times 16$ magnifications. To obtain a full view of the aortic arch, pericardium and thymus were removed. The aorta was then freed from the surrounding fatty tissue and cut at the arch, just above the origin of the anonymous artery, which was also cut. Immediately, an opening to the thoracic inferior vena cava was performed. The insertion of a 22G cannula into the opening was then completed and the heart was flushed with 20–25 mL of saline solution at 4°C, using little pressure. Perfusion was discontinued when the heart stopped beating and the flow coming from the aorta became clear. The pulmonary artery (PA) was divided close to the bifurcation trying to ensure maximum length, entering with one blade of the micro scissors underneath the vas. The PA was then gently held with the ring tip micro forceps and was divided from the right ventricle with the micro spring scissors, removing some muscle as well.

Back Table

The PA root was placed on a gauze moistened with cold saline and the pulmonary root was inspected under the operating microscope. Any abundant surrounding tissue was removed. Only 1 mm of ventricular muscle was left, while the length of the vas was set to 5 mm. The homograft was used immediately for the recipients entering FRESH group, or sent to the lab for the tissue decellularization process and implanted one-week later to the recipients entering the DECELL group.

Generation of Pulmonary Homograft Decellularized Matrix

The pulmonary homograft was washed in sterile phosphate buffered saline (PBS) 1 \times and conserved in PBS containing 1% penicillin-streptomycin solution. Afterwards, the homograft was treated with the detergent-enzymatic treatment (DET) protocol. Briefly, each DET cycle was composed of deionized water at 4°C for 24 h, 4% sodium deoxycholate (Sigma Aldrich Srl, Milan, Italy) at room temperature (RT) for 4 h, and 2000 kU DNase-I (Sigma Aldrich Srl, Milan, Italy) in

1 M NaCl (Sigma Aldrich Srl, Milan, Italy) at RT for 3 h, after washing in water [11]. Afterwards, the DPH was washed for 2 days in deionized sterile water. Decellularized tissue was stored at 4°C in PBS 3% penicillin/streptomycin (Thermo Scientific, Waltham, USA), or immediately used.

We also investigated the number of cycles necessary to obtain complete cell removal using from one to four DET cycles.

DNA Isolation and Quantification

To assess total DNA content within the homograft, specimen was treated using Dneasy Blood & Tissue kit (Qiagen Srl, Milan, Italy) following manufacturer's instructions. DNA samples were then quantified using Nanodrop 2000 spectrophotometer (Thermo Scientific).

Initial Stage of Recipient Operation

The animal was placed supine on a cork tray with its caudal part towards the surgeon, shaved along the midline for 2 cm width from the sternum to 1 cm above the genital area, and disinfected. At this point, we covered the recipient with transparent plastic kitchen film to avoid heat dispersion or wetting of the animal during surgery. A median longitudinal incision was performed. Two mini retractors were used to keep the abdomen open. A gauze soaked with 39°C saline was inserted in the animal's right side, and the intestines were pulled out and wrapped in the gauze. During surgery, it was our good practice to occasionally moisten the intestines with a syringe containing 39°C saline, to prevent hypothermia, a common critical condition in rodents. The graft was placed halfway between the renal vessels and the iliac bifurcation. The posterior parietal peritoneum of this area, covering the major abdominal vessels, was stripped using two cotton buds, and the portion of interest of the abdominal aorta (AA) was cleaned from the fat. Only a small piece of fat was left over the AA, to facilitate the grasp on the vessel. We separated the AA from the AVC, without running any unnecessary risks: the entire procedure was performed by pulling on the anterior wall of the AA, while the curved forceps were used to open a passage and pass a loop of 2/0 silk (Johnson & Johnson Medical SpA) posterior to the AA. With the aid of this loop, it was easy to lift the vessel and separate AA from AVC. Eventual lumbar arteries generating from the AA area of interest were ligated with silk 6/0, and divided. The animal was rotated 90° counterclockwise (head to the operator's left), so the vessel was placed horizontally across the microscopic field. The two Yasargil clips were put in the AA at a 1.5 cm distance from each other (Figure 1A), and the AA was transected at the middle

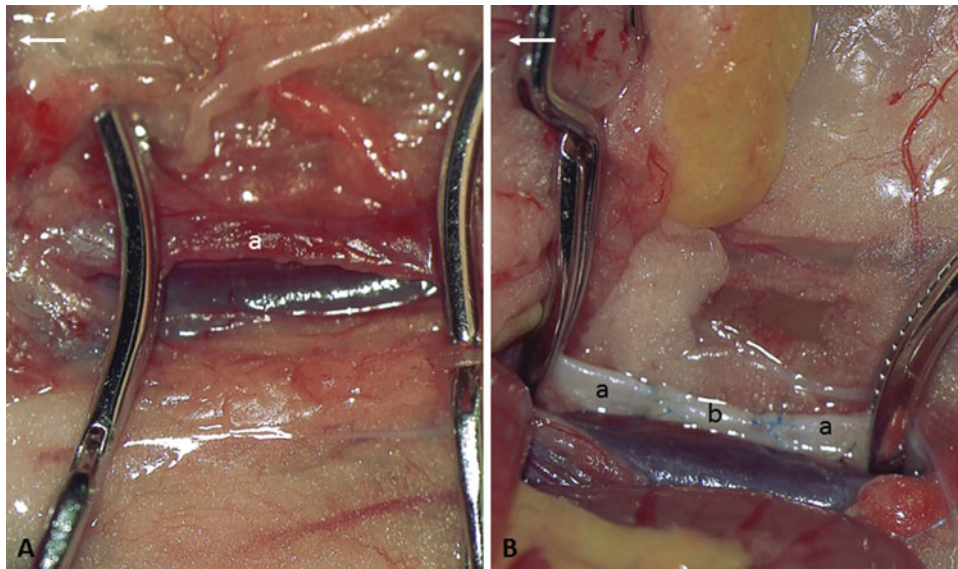


FIGURE 1 A) Positioning the two Yasargil clips in the abdominal aorta. B) End of the anastomosis; (←) head of the animal; (a) abdominal aorta; (b) decellularized pulmonary homograft.

point with a single, decisive cut. To remove any clots, the AA openings were irrigated with saline solution with heparin 1 IU/mL. The aortic stumps were cleaned from any adventitial debris with a sleeve amputation of the vessel. In the case of the SHAM group, at this point we re-anastomosed with 10/0 Prolene the AA in the classic way. Regarding the other two experimental groups, we proceeded as follows.

Pulmonary Homograft Implant

We used a 10/0 Prolene running suture for the end-to-end anastomosis of the homograft with the AA. We began on the side of our dominant hand, so the distal

anastomosis was performed first. We put two stay sutures at halfway points of the circumference, one in front of other. The same maneuver was repeated proximally, to fix the homograft with the AA. The sutures were applied using a recipient-to-graft out-in/in-out sequence, and tied with a double half hitch completed with a square knot. Sutures were left under traction induced by plastic clips. A running suture of 5-6 stitches was performed firstly on the anterior row (Figure 2A). We locked the last stitch to prevent anastomosis narrowing, due to any over-tight knotting with the stay suture. Also after completing the anterior row of the anastomosis proximally; taking care not to include any leaflet in the suture line, both Yasargil clips were rotated 180°. The posterior wall of

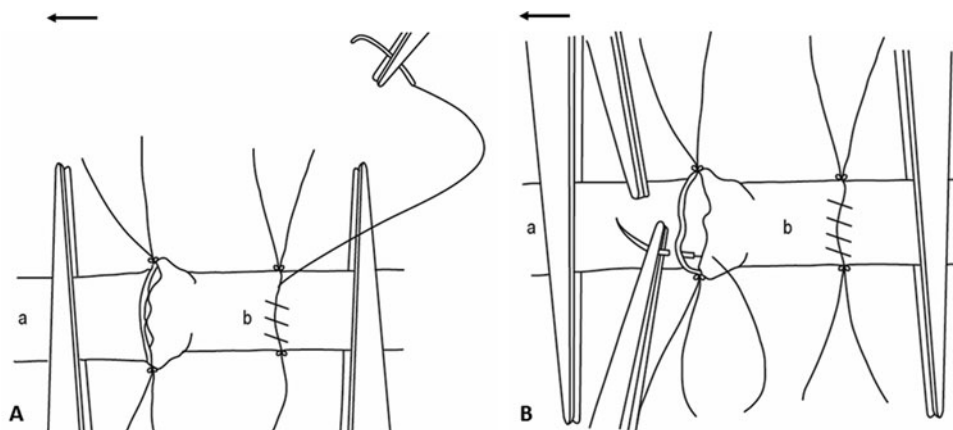


FIGURE 2 A) Anastomosis of the anterior wall: two stay sutures put halfway of the circumference in front of each other, distally and proximally, to fix the homograft to the abdominal aorta; the distal anastomosis was performed first. B) Anastomosis of the posterior wall, after Yasargil clips were rotated 180°, was completed in the same fashion as the anterior wall (see text for details); (←) head of the animal; (a) abdominal aorta; (b) decellularized pulmonary homograft.

the anastomosis was thus completed in the same fashion as the anterior wall, beginning distally, and then proximally (Figure 2B). The distal clip was released a couple of times allowing the homograft to be filled with retrograde blood (low-pressure flow). In this way, we checked for blood leakage and put supplementary *ad hoc* single sutures before the final declamping (Figure 1B).

Final Stage of Recipient Operation

The patency of the homograft was assessed and two strips of gelatin sponge were applied over the suture lines on both sides of the graft. To help hemostasis, some pressure was exercised for a few seconds with two cotton buds. If everything had gone smoothly, no important blood loss from the anastomosis occurred and the pulmonary homograft quickly regained its normal color and pulsed like the rest of the AA. The intestines were restored to their proper place and the abdomen was closed in two layers with a 4/0 running suture.

Other Procedures

A single dose of intramuscular Gentamycin (Gentalyn[®], MSD Italia Srl., Rome, Italy) 5 mg/kg was administered during surgery. Moreover, 5 mL of warm saline solution was administered subcutaneously at the back of the animal for hydration. The animal was then placed under a heating lamp and visually monitored until it woke up, which usually takes up to 5 minutes after suspending anesthesia. The animal was left to recover at a room temperature of 22–24°C, with immediate, unrestricted access to food and water. Intramuscular tramadol, at a dose of 5 mg/kg, was used as an analgesic twice daily for the first 48 hours after surgery. Afterwards, the recipient's health status and body weight were monitored daily.

Ultrasonographic and Doppler Evaluation

All animals underwent abdominal ultrasonographic evaluation performed at 15 days after surgery, using a high-resolution echo machine with a 13–24 Mhz probe (Vevo[®] 2100, VisualSonics, Toronto, Canada). Animals were abdomen shaved and anesthetized with 3% sevoflurane, and temperature controlled anesthesia was maintained with 1.5% sevoflurane. Two-dimensional cine loops of abdominal aorta were recorded. Native aorta diameter was measured upstream (diameter pre implant) and downstream (diameter post implant). The implanted valve diameter was measured from B-mode cine loops. Doppler evaluation of the abdominal aortic blood flow upstream and

downstream of the implanted valve was performed from an abdominal longitudinal view. The following aortic parameters were measured: peak systolic velocity (PSV) upstream (pre) and downstream (post) the implanted valve; the percentage of variation was also calculated: $[(PSV \text{ post} - PSV \text{ pre})/PSV \text{ post}] \%$. In the SHAM group, the abdominal aortic evaluation (diameter and Doppler flow) was performed immediately at the origin of the renal arteries and close to the iliac bifurcation. A single operator performed ultrasonographic and Doppler evaluation.

Morphological Evaluation

After euthanasia, at the time point of 15 days post-surgery, samples of the pulmonary homografts, together with a portion of AA and aortic arteries were fixed in 4% formaldehyde, in pH 7.2 phosphate 0.05% buffer, and sent to the pathological anatomy for morphological evaluation. After gross and X-ray examination, the samples were sectioned in longitudinal orientation. Thereafter, the samples were dehydrated in crescent ethanol series, paraffin embedded, and 4- to 5- μm -thick sections were stained with hematoxylin-eosin to detect cells (nucleus and cytoplasm), Weigert-Van Gieson to evidence collagen and elastin, Heidenhein modified Azan Mallory for both cells and fibrillar extracellular matrix, Alcian PAS for ground substance extracellular matrix. To evidence autologous origin repopulation cells, other sections of pulmonary homografts were incubated with a rabbit polyclonal anti GFP antibody (Abcam, Cambridge, UK) followed by Envision HRP Kit Complex (Dakocytomation, Glostrup, Denmark).

Statistical Analysis

Ultrasonographic and Doppler evaluation data are expressed as mean \pm standard error. For a comparison between groups, the null hypothesis was tested by a single factor analysis of variance (ANOVA) for multiple groups or unpaired *t*-test for two groups. Statistical significance ($p < 0.05$) between the experimental groups was determined by the Fisher method of analysis for multiple comparisons.

RESULTS

Surgery

Overall, 17 subsequent, first series, surgical procedures were performed by a single surgeon with experience in experimental microsurgery [12]. The median total recipient operating time (skin-to-skin) was 148 minutes (range: 135–175 minutes). We had a surgery success

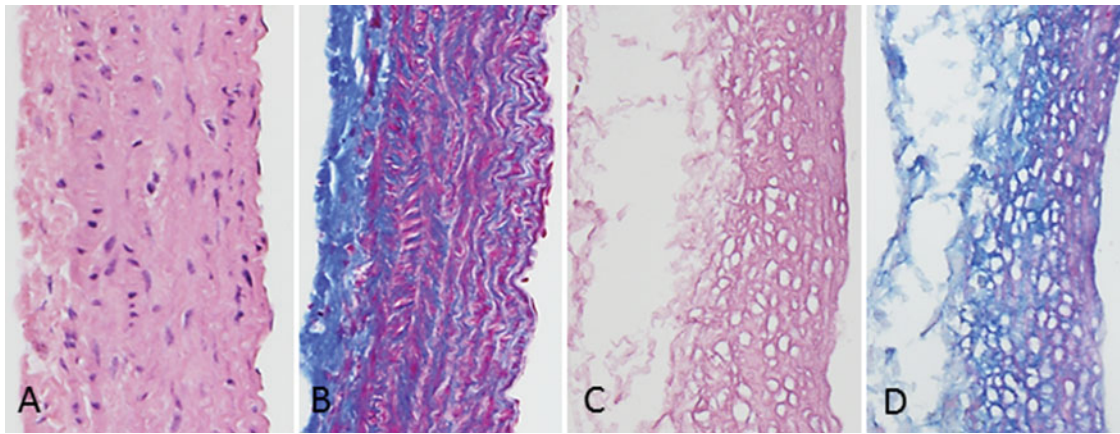


FIGURE 3 Native pulmonary homograft (A–B). Wall appears rich in cells with regular endothelial lining. C–D) Unimplanted decellularized pulmonary homograft with the scaffold of collagen bundle well preserved. All cells disappeared. A, C) Hematoxylin-eosin, 125 \times original magnification; B, D) Azan Mallory Heidenhein modified, 125 \times original magnification.

rate of 82% (14/17 animals), or 77% if we only consider the implanted homografts. No late surgical failure occurred. The early surgical failures, occurring at the beginning of our experience, included three recipients, who died between 40–72 hours postoperatively due to aortic thrombosis in the site of implantation.

Decellularization Protocol: Pre-Surgery Molecular and Morphological Evaluation

After three cycles, cell loss in the tissue was complete. The tissue acquired a white, almost transparent appearance. Residual DNA content in the tissue was 5 ng/ μ l, with a removal of DNA content greater than 95%, without differences between the third and the fourth cycles. For this reason, the DET protocol was settled with three cycles. Histological analyses demonstrated that while the fresh pulmonary homograft appeared normally populated with cells (Figure 3A–B), in the DPH, the decellularization appeared complete with intact extracellular matrix (Figure 3C–D).

Ultrasonographic and Doppler Follow up

In SHAM animals, mean aortic diameter was 1.6 ± 0.2 mm downstream of the origin of the renal arteries and 1.2 ± 0.2 mm upstream of the iliac bifurcation. In the DECELL group, aortic diameters were 1.43 ± 0.13 mm (diameter pre implant) and 1.38 ± 0.08 mm (diameter post implant), while the “valve implant” diameter was 3.1 ± 0.08 mm (+62%, as compared to the diameter pre implant). In the FRESH group, aortic diameters were 1.57 ± 0.15 mm (diameter pre implant) and 1.40 ± 0.07 mm (diameter post implant), while the “valve implant” diameter was 3.6 ± 0.2 mm (+55%, as compared to the diameter pre implant).

In the SHAM group, a small increase (+0.08%) was observed in aortic PSV upstream of the iliac bifurcation (1240 ± 432 mm/s) as compared to PSV downstream of the renal arteries (1274 ± 274 mm/s). In the FRESH group, the mean increase in PSV was 49% (PSV pre = 1060 ± 688 mm/s; PSV post = 2084 ± 360 mm/s), while in the DECELL group the mean increase in PSV was 28% (PSV pre = 1320 ± 89 mm/s; PSV post = 1795 ± 58 mm/s). (Figure 4). The difference between the two groups was not statistically significant because of the small number of animals.

Post-Operative Morphological Evaluation

At 15 days from surgery, the implanted fresh pulmonary homografts showed a massive tissue inflammatory reaction (Figure 5A–B) with regular elastic fibers (Figure 5C), while DPH showed cell repopulation in the outer media wall and partial endothelial lining in absence of rejection (Figure 5E). Focal intimal hyperplasia was also detected (Figure 5F), while elastic fibers were regular, but rather close to one another in the luminal part of the media because of the absence of cells (Figure 5G). The repopulation cells were all GFP+ (Figure 5H), in comparison with fresh pulmonary homografts in which only recipient inflammatory cells are GFP+ (Figure 5D).

DISCUSSION

At present, cardiovascular diseases represent the most significant cause of death in Europe. Many of the acquired and congenital heart diseases can necessitate heart valve replacement; however, none of the currently available heart valve substitutes is considered “ideal.” For this reason, various investigative work on

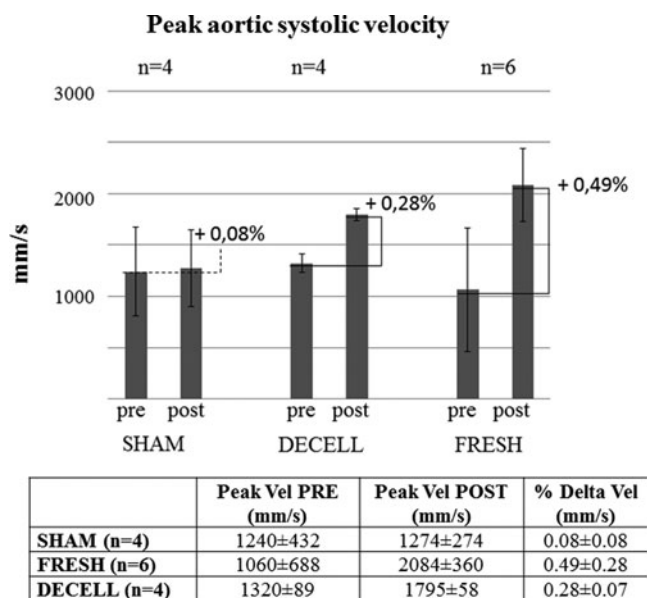


FIGURE 4 Graphic representation of the peak aortic systolic velocity upstream and downstream the implanted homograft; in SHAM animals, the peak aortic velocity was measured at the origin of the renal arteries and immediately close to the iliac bifurcation. SHAM = sham-operated group; DECELL = decellularized homograft group; FRESH = fresh homograft group. Peak Vel PRE: peak aortic systolic velocity measured upstream the implanted homograft; Peak Vel POST: peak aortic systolic velocity measured downstream the implanted homograft; % Delta Vel: difference between peak aortic systolic velocity upstream and downstream the implanted homograft, calculated in percentage. Data are expressed as mean \pm standard error.

this matter has been done in several animal models [13, 14]. The most interesting results are derived from the use of non-cryopreserved homografts, chemically treated to inactivate adhering microorganisms and viruses [15] and, in addition, decellularized to eliminate the DNA content and leave only connective tissue [16]. Studies in large animals have shown some important inherent limitations: they are costly, ethically demanding and only a limited number of animals can be used. On the other hand, rodent models, certainly more surgically challenging, can be extremely helpful and offer several advantages, such as facility of organization, bigger numbers, short and long-term results achieved in a relatively short period and a wide range of transgenic animals available.

In the current literature, only one report mentions the heterotopic pulmonary homograft to abdominal aorta technique [17], while no reports include a rodent model like the one we have developed and no descriptions of the employed technique have ever been published. In this report, we describe in detail our small animal model in order to disseminate the necessary expertise to study the performance of a heterotopic DPH as a simple matrix for autologous cell self-seeding. All the necessary steps have been reported to facilitate the procedure for surgeons and laborato-

ries who are willing to start working with this model. Several details provided—from the donor pulmonary artery root harvesting to its implantation in the recipient abdomen—aim to be of assistance to surgeons, helping them to improve their results. The reported surgical technique is safe, reproducible, and constitutes an excellent opportunity for trainees on gaining familiarity with microvascular and experimental surgery. The principal technical hint is the use of continuous suturing to perform the end-to-end anastomosis. While microsurgery textbooks describe separate stitches for this kind of anastomosis, we prefer continuous suturing because it better tightens the DPH and it becomes easier to reduce the size difference between the DPH and the recipient aorta.

The DPH offers the advantage of having a substrate that perfectly mimics architecture and organization of the native tissue and presents the same biochemical composition, cell homing activation, biomechanical and angiogenic properties. By using our DET protocol, we have been able to obtain a well-preserved valvular ECM that maintained the same protein composition and distribution of fresh tissue, but with depletion of nuclei content. Drastic decrease in DNA quantity and cell number in the treated tissue is a crucial outcome in decellularization methods and here we obtained significant cell depletion in order to avoid any *in vivo* immune-related rejection of the scaffold. Decellularization was evidenced with histological analysis: cell loss was quite effective, but extracellular matrix was preserved.

Replacement of the diseased aortic valve by the autologous pulmonary valve autograft (the so called Ross procedure, proposed for the first time since 1962), is still considered a clinically effective procedure in children with aortic valve disease [18]. Therefore, the use that we have made of the pulmonary homograft in a heterotopic position under systemic pressure “mimics” the clinical use of the pulmonary valve in an aortic position. Furthermore, experimental studies on valve decellularization have been extensively published in recent years and their use is reported in a growing number of groups of patients, but no studies on DPH in a systemic position under increased pressure stress has, to our knowledge, yet been performed. We intended to use this “extreme” rodent model to study the valvular performance and regenerative capacity in this particular hemodynamic condition.

Ultrasonographic evaluation is the first-line imaging study for the postoperative evaluation and follow up of patients with diseases of the abdominal vessels. It provides a very accurate measurement of the aortic diameters, is a well-known sensitive and specific first line evaluation in abdominal aorta diseases and is useful for identifying stenosis and occlusions [19]. Doppler evaluation is widely used in echocardiographic assessment of cardiac valvular disease such as stenosis and/or insufficiency and is the recommended

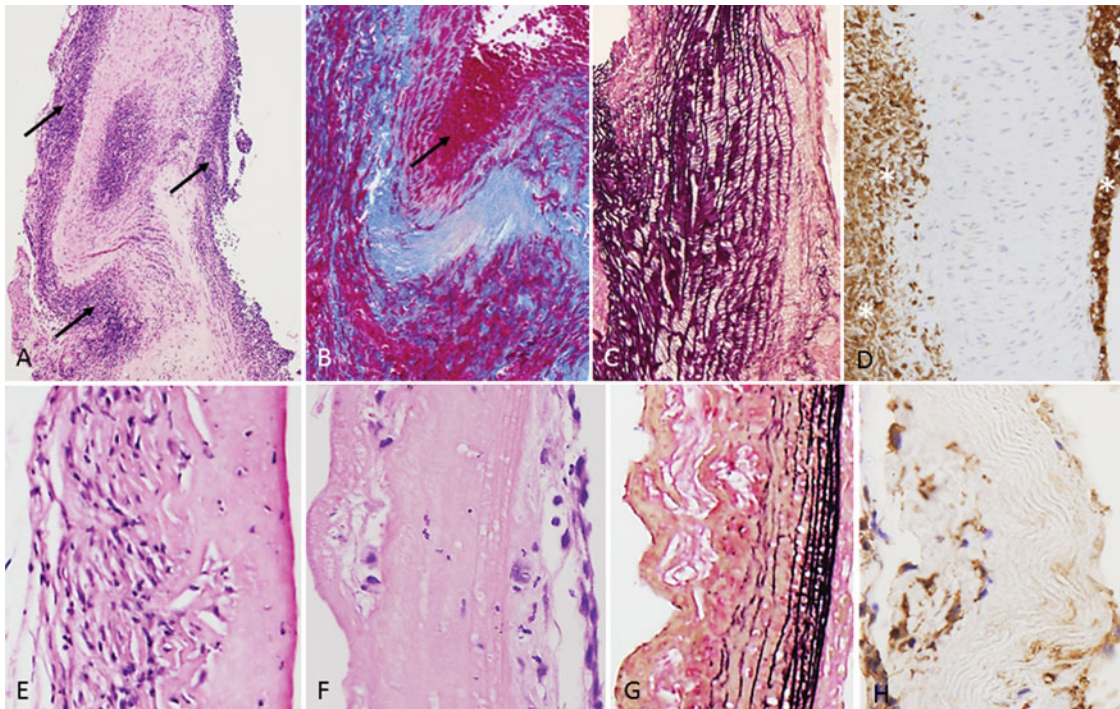


FIGURE 5 Fresh pulmonary homograft at 15 days from the implant (A–D): a massive tissue inflammatory reaction is visible (A, B, arrows). Elastic fibers are regular (C) and only recipient inflammatory cells are GFP positive (D, asterisks). E–H) Decellularized pulmonary homograft at 15 days from the implant: a new population of cells is visible in the outer media wall and in the endothelial lining in absence of rejection (E). Focal intimal hyperplasia was also detected (F). Elastic fibers are regular, but rather close to one another in the luminal part of the media (G); the repopulation cells are GFP positive (H). A, E, F) Hematoxylin-eosin: A) 50× original magnification; E, F) 125× original magnification; B) Azan Mallory Heidenhein modified, 200× original magnification; C, G) Weigert Van Gieson: C) 125× original magnification; G) 200× original magnification; D, H) anti rabbit polyclonal GFP: D) 125× original magnification; H) 320× original magnification.

method for the evaluation of prosthetic valves [20]. High-resolution ultrasound machines allow a sensitive and specific evaluation of abdominal aorta in rodents [21]. In this study, the ultrasonographic assessment of the distal aorta allowed a non-invasive, dynamic, *in vivo* evaluation of the implanted homograft. The difference in PSV upstream (pre) with downstream (post) pulmonary homograft in the FRESH group, in comparison with the DECELL group (49% versus 28%, respectively), was probably due to the presence of a “resistive element” (valve). Though the difference between the two groups was not statistically significant, data suggest that the DPH is a “less resistive element.” Our hypothesis is that graft rejection favors inflammation, fibrosis and/or thrombosis, thus increases intra-graft resistance with a subsequent increase in PSV post implant. To evaluate the “accuracy” of Doppler ultrasonography in detecting rejection, further experiments need to be performed.

The pathological evaluation at a time point of 15 postoperative days, aimed to demonstrate morphologically the complete loss of the cell population in unimplanted DPH in comparison with the fresh controls and the appearing of the new cell repopulation

in the implanted DPH, especially in the outer portion of the media (adventitial side), as reported in previous studies [22, 23]. The safety of the method was demonstrated by preserved extracellular matrix with intact collagen, elastin, and ground substance. No rejection reaction occurred in DPH implants; arterial wall was partially repopulated, mainly in adventitial side of the media. Experimental evidence suggests an autologous origin of the repopulation cells (endothelial and mesenchymal cells) contributing to the recruitment of cells [24, 25]. Circulating bone-marrow-derived endogenous cells can be recruited by adhering to intravascular surfaces via a pathway similar to inflammatory cells to the endothelium during physiological inflammation [26, 27].

In conclusion, the heterotopic DPH implantation technique in rats is a feasible and reproducible model, although it necessitates a learning curve and a meticulous technique. The present model can be fundamental for building a valid study model of the DPH implanted in a heterotopic position and for any further exploitation of the subject. In a short-term follow up, the implanted DPH showed autologous repopulation in absence of rejection.

ACKNOWLEDGMENTS

This work was supported by Associazione Un Cuore Un Mondo Padova Onlus. The authors also thank Erika Borsetto, whose contribution and support made this study possible.

Declaration of interest: The authors report no conflicts of interest. The authors alone are responsible for the content and writing of the paper.

REFERENCES

- [1] van Geemen D, Soares AL, Oomen PJ et al. Age-dependent changes in geometry, tissue composition and mechanical properties of fetal to adult cryopreserved human heart valves. *PLoS One*. 2016;11:e0149020.
- [2] Cohn LH, Collins JJ Jr, Di Sesa VJ et al. Fifteen-year experience with 1678 Hancock porcine bioprosthetic heart valve replacements. *Ann Surg*. 1989;210:435–442; discussion 442–443.
- [3] Jamieson WR, Munro AI, Miyagishima RT et al. Carpentier-Edwards standard porcine bioprosthesis: clinical performance to seventeen years. *Ann Thorac Surg*. 1995 Oct;60(4):999–1006; discussion 1007.
- [4] Hopkins R. Cardiac surgeon's primer: tissue-engineered cardiac valves. *Semin Thorac Cardiovasc Surg Pediatr Card Surg Annu*. 2007:125–135. Review.
- [5] Theodoridis K, Tudorache I, Calistru A et al. Successful matrix guided tissue regeneration of decellularized pulmonary heart valve allografts in elderly sheep. *Biomaterials*. 2015;52:221–228.
- [6] Flaumenhaft R, Moscatelli D, Saksela O et al. Role of extracellular matrix in the action of basic fibroblast growth factor: matrix as a source of growth factor for long-term stimulation of plasminogen activator production and DNA synthesis. *J Cell Physiol*. 1989;140:75–81.
- [7] Neumann A, Sarikouch S, Breyman T et al. Early systemic cellular immune response in children and young adults receiving decellularized fresh allografts for pulmonary valve replacement. *Tissue Eng Part A*. 2014;20:1003–1011.
- [8] Baraki H, Tudorache I, Braun M et al. Orthotopic replacement of the aortic valve with decellularized allograft in a sheep model. *Biomaterials*. 2009;30:6240–6246.
- [9] Della Barbera M, Valente M, Basso C et al. Morphologic studies of cell endogenous repopulation in decellularized aortic and pulmonary homografts implanted in sheep. *Cardiovasc Pathol*. 2015;24:102–109.
- [10] Grauss RW, Hazekamp MG, van Vliet S et al. Decellularization of rat aortic valve allografts reduces leaflet destruction and extracellular matrix remodeling. *J Thorac Cardiovasc Surg*. 2003Dec;126(6):2003–2010.
- [11] Piccoli M, Urbani L, Alvarez-Fallas ME et al. Improvement of diaphragmatic performance through orthotopic application of decellularized extracellular matrix patch. *Biomaterials*. 2016;74:245–255.
- [12] Dedja A, Zaglia T, Dall'Olmo L et al. Hybrid cardiomyocytes derived by cell fusion in heterotopic cardiac xenografts. *FASEB J*. 2006;20:2534–2536.
- [13] Schmitt B, Spriestersbach H, O H-Ici D et al. Percutaneous pulmonary valve replacement using completely tissue-engineered off-the-shelf heart valves: six-month in vivo functionality and matrix remodelling in sheep. *Euro Intervention*. 2016;12:62–70.
- [14] Kim DH, Park HK, Park YH et al. Degenerative calcification of pericardial bioprostheses: comparison of five implantation methods in a rabbit model. *J Heart Valve Dis*. 2015;24:621–628.
- [15] Sarikouch S, Horke A, Tudorache I et al. Decellularized fresh homografts for pulmonary valve replacement: a decade of clinical experience. *Eur J Cardiothorac Surg*. 2016;50:281–290.
- [16] Tudorache I, Cebotari S, Sturz G et al. Tissue engineering of heart valves: biomechanical and morphological properties of decellularized heart valves. *J Heart Valve Dis*. 2007;16:567–573; discussion 574.
- [17] Kneebone JM, Lupinetti FM. Procollagen synthesis by fresh and cryopreserved rat pulmonary valve grafts. *J Thorac Cardiovasc Surg*. 2000;120:596–603.
- [18] Ross D, Jackson M, Davies J. The pulmonary autograft—a permanent aortic valve. *Eur J Cardiothorac Surg*. 1992;6:113–116; discussion 117.
- [19] Battaglia S, Danesino GM, Danesino V et al. Color Doppler ultrasonography of the abdominal aorta. *J Ultrasound*. 2010Sep;13(3):107–117.
- [20] Zoghbi WA, Chambers JB, Dumesnil JG et al. American Society of Echocardiography's Guidelines and Standards Committee; Task Force on Prosthetic Valves; American College of Cardiology Cardiovascular Imaging Committee; Cardiac Imaging Committee of the American Heart Association; European Association of Echocardiography; European Society of Cardiology; Japanese Society of Echocardiography; Canadian Society of Echocardiography; American College of Cardiology Foundation; American Heart Association; European Association of Echocardiography; European Society of Cardiology; Japanese Society of Echocardiography; Canadian Society of Echocardiography. Recommendations for evaluation of prosthetic valves with echocardiography and Doppler ultrasound: a report from the American Society of Echocardiography's Guidelines and Standards Committee and the Task Force on Prosthetic Valves, developed in conjunction with the American College of Cardiology Cardiovascular Imaging Committee, Cardiac Imaging Committee of the American Heart Association, the European Association of Echocardiography, a registered branch of the European Society of Cardiology, the Japanese Society of Echocardiography and the Canadian Society of Echocardiography, endorsed by the American College of Cardiology Foundation, American Heart Association, European Association of Echocardiography, a registered branch of the European Society of Cardiology, the Japanese Society of Echocardiography, and Canadian Society of Echocardiography. *J Am Soc Echocardiogr*. 2009Sep;22(9):975–1014; quiz 1082–1084.
- [21] Knipp BS, Ailawadi G, Sullivan VV et al. Ultrasound measurement of aortic diameters in rodent models of aneurysm disease. *J Surg Res*. 2003 Jun 1;112(1):97–101.
- [22] Cebotari S, Tudorache I, Ciubotaru A et al. Use of fresh decellularized allografts for pulmonary valve replacement may reduce the reoperation rate in children and young adults: early report. *Circulation*. 2011Sep13;124(11 Suppl):S115–S123.
- [23] Quinn RW, Hilbert SL, Bert AA, et al. Performance and morphology of decellularized pulmonary valves implanted in juvenile sheep. *Ann Thorac Surg*. 2011 Jul;92(1):131–137.

- [24] Deb A, Wang SH, Skelding K et al. Bone marrow-derived myofibroblasts are present in adult human heart valves. *J Heart Valve Dis.* 2005 Sep;14(5):674–678.
- [25] Armstrong EJ, Bischoff J. Heart valve development: endothelial cell signaling and differentiation. *Circ Res.* 2004 Sep 3;95(5):459–470. Review.
- [26] Sata M, Fukuda D, Tanaka K et al. The role of circulating precursors in vascular repair and lesion formation. *J Cell Mol Med.* 2005 Jul-Sep;9(3):557–568. Review.
- [27] Frid MG, Kale VA, Stenmark KR. Mature vascular endothelium can give rise to smooth muscle cells via endothelial-mesenchymal transdifferentiation: in vitro analysis. *Circ Res.* 2002 Jun 14;90(11):1189–1196.